LETTER

doi:10.1038/nature12882

Australian tropical cyclone activity lower than at any time over the past 550–1,500 years

Jordahna Haig[1], Jonathan Nott[1] & Gert-Jan Reichart[2,3]

The assessment of changes in tropical cyclone activity within the context of anthropogenically influenced climate change has been limited by the short temporal resolution of the instrumental tropical cyclone record[1,2] (less than 50 years). Furthermore, controversy exists regarding the robustness of the observational record, especially before 1990[3–5]. Here we show, on the basis of a new tropical cyclone activity index (CAI), that the present low levels of storm activity on the mid west and northeast coasts of Australia are unprecedented over the past 550 to 1,500 years. The CAI allows for a direct comparison between the modern instrumental record and long-term palaeotempest (prehistoric tropical cyclone) records derived from the $^{18}O/^{16}O$ ratio of seasonally accreting carbonate layers of actively growing stalagmites. Our results reveal a repeated multicentennial cycle of tropical cyclone activity, the most recent of which commenced around AD 1700. The present cycle includes a sharp decrease in activity after 1960 in Western Australia. This is in contrast to the increasing frequency and destructiveness of Northern Hemisphere tropical cyclones since 1970 in the Atlantic Ocean[6–8] and the western North Pacific Ocean[6,7]. Other studies project a decrease in the frequency of tropical cyclones towards the end of the twenty-first century in the southwest Pacific[7,9], southern Indian[9,10] and Australian[11] regions. Our results, although based on a limited record, suggest that this may be occurring much earlier than expected.

Trend analysis of the instrumental tropical cyclone record has proven difficult owing to errors associated with changes in observational techniques (leading to inaccurate intensity estimates and storm counts in the recent past), detection issues, data homogeneity issues[3,6,12] and inconsistent procedures between and within agencies[1,3–5]. As a result, differentiating natural variability from anthropogenically induced change is complicated; this may also explain to a certain extent the disparity between current trend estimates[6,13].

In an effort to remedy this we have developed a new technique, which calibrates high-resolution, long-term palaeorecords of tropical cyclone activity against the instrumental tropical cyclone record. This scale allows for a direct comparison between the past and present, and enables an examination of tropical cyclone climatology at higher temporal resolution and on annual, decadal or millennial scales simultaneously, without the need to interpolate or extrapolate to account for missing data. Our index, CAI, is based on tropical cyclone activity indices developed by the National Oceanic and Atmospheric Administration and others, which describe the severity of a season in terms of the number of storms, their intensity (V_{max}), their size (R_{max}) and their longevity. These indices include the accumulated cyclone energy index[14], the revised accumulated cyclone energy index[15], the power dissipation index[6] and the hurricane intensity index[16] (Methods). CAI is the average accumulated energy expended over the tropical cyclone season within range of the site, accounting for the number of days since genesis and the intensity and size of the storm relative to its distance from the site at each point along its track (Fig. 1):

$$\mathrm{CAI} = \frac{1}{N}\sum_{n=1}^{N} K_{n,t}$$

where $K_{n,t} = (K_t + K_{t-1})_n$, $K_t = V_{max}^3(t)R_{max}(t)/d(t)$, N is the number of storms within the season, n enumerates the individual storms, t denotes time along the storm track (recorded at 6-h intervals), $d(t)$ is the distance from the site in kilometres at time t, $V_{max}(t)$ is the maximum 10-min-mean wind speed in metres per second at time t, and $R_{max}(t)$ is the radius of maximum wind in kilometres at time t.

Tropical cyclones produce precipitation that is depleted in the heavier oxygen isotope (^{18}O) by >6‰ relative to average monsoonal precipitation, owing to the recycling of water within the system, high condensation efficiency and large size and longevity of such cyclones as intense convective systems[17]. The resulting $\delta^{18}O$ content (expressed as $\delta^{18}O = [(^{18}O/^{16}O)_{sample}/(^{18}O/^{16}O)_{standard} - 1)] \times 1{,}000‰$) of tropical cyclone precipitation at a site is influenced by a number of factors, including the number of days since genesis (that is, rainout) and the intensity of the storm, its source region[18] and the distance of its centre from the sampling path. Because tropical stalagmites are archives of monsoonal $\delta^{18}O$, signatures of past tropical cyclones are also recorded within the $\delta^{18}O$ of their carbonate layers, typically within 400 km of the storm centre[19,20].

Two cylindrical stalagmites were collected from regions in Queensland and Western Australia prone to tropical cyclones (Chillagoe in Queensland, stalagmite CH-1; Cape Range in Western Australia, stalagmite CR-1). Both show a continuous, uninterrupted record of distinct seasonal growth banding composed of alternating layers of dark and light calcite corresponding to wet- and dry-season deposition. No visible hiatuses were present. The first 1,500 wet-season (dark-calcite) layers were analysed for their carbonate $\delta^{18}O$. Observed differences between maxima and minima in $\delta^{18}O$ over the time period are 4.38‰ (CH-1) and 5.81‰ (CR-1). In both locations, $\delta^{18}O$ is highly variable between wet seasons: yearly differences range from −1.6‰ to 2.08‰ in CH-1 and from −2.5‰ to 2.2‰ in CR-1, which are too large to be explained by a cave temperature effect because this would imply a shift in annual temperatures of 6–8 °C (ref. 21). Neither CR-1 nor CH-1 exhibits a significant relationship between $\delta^{18}O$ and the seasonal rainfall total, the annual rainfall total or the number of rain days at the corresponding site ($\rho < 0.07$ (Spearman's rho), $P > 0.5$ for CR-1; $\rho < -0.08$, $P > 0.2$ for CH-1). In the absence of cave temperature or rainfall 'amount effects' we conclude that rainfall composition rather than cave temperature and rainfall amount or frequency, or both, influences the resulting $\delta^{18}O$. However, periods of non-tropical cyclone rainfall and changes in the strength of the Australian–Indonesian monsoon are expected to dilute the cave reservoir. Stalagmite monsoon records from latitudes below 8° S (which are therefore less influenced by tropical cyclone activity) show variations of up to 0.7‰–1.2‰ (ref. 22) over a 1,500-year period. These values are considerably less than the 4‰–6‰ variation between the maxima and minima and the 1.6‰–2.5‰ seasonal variation within the stalagmite $\delta^{18}O$ presented here. Nevertheless, we account for the monsoonal contribution to $\delta^{18}O$ using empirical methods for determining the average value of precipitation $\delta^{18}O$ VSMOW (that is, $\delta^{18}O$ where the standard is Vienna standard mean ocean water) at both sites, and we account for centennial scale changes

[1]Earth and Environmental Sciences, James Cook University, Cairns, Queensland 4870, Australia. [2]Department of Geochemistry, Utrecht University, Utrecht 3508 TA, The Netherlands. [3]Geology Department, Royal Netherlands Institute for Sea Research, Den Hoorn (Texel) 1797 SZ, The Netherlands.

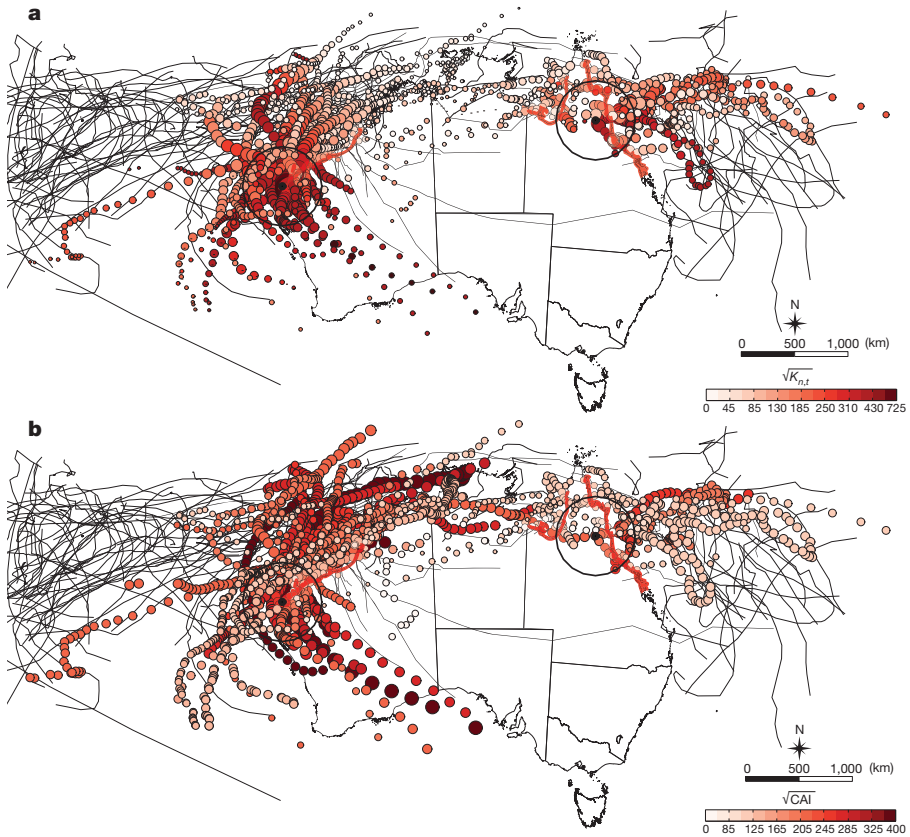

Figure 1 | Site map showing the four-stage calculation of CAI. Chillagoe and Cape Range (black points) are shown with the 400-km radius around each study site. Tropical cyclones whose tracks did not lie within the study area during the training period in Queensland and Western Australia are shown in black. Red shading indicates the coastlines most prone to tropical cyclones in both states. **a**, Tropical cyclones from the 1990–2010 training period and their corresponding K_t value (point size), showing the influence of V_{max}, R_{max} and distance; cumulative $K_{n,t}$ values are shown in colour. **b**, Point size indicates K_n (individual storm averages) calculated from **a** and subsequent seasonal CAI values (gradated colour).

in monsoonal activity using published Australian–Indonesian monsoon records[22] (Methods).

Figure 2 shows the relationship between CAI, calculated from 'best tracks' in the recently updated tropical cyclone database for the region[23], and the de-trended $\delta^{18}O$ (that is, $\delta^{18}O_A$) for the corresponding period 1990–2010. The model predicts CAI well in 63% of cases ($P < 0.001$) within the $\delta^{18}O_A$ range of −6.37‰ to −1.03‰. That being the case, larger negative excursions in $\delta^{18}O$ correlate with higher CAI values. Although this range is representative of the data obtained from the whole series (2,276 measurements in total), $\delta^{18}O_A$ values that fall outside the model range may not be calculated effectively. However, $\delta^{18}O_A$ values exceeded or fell below the range in only 28 or 88 cases, respectively. Of these, only four were more than 1 s.d. outside the range. Each series was standardized before statistical analysis. No patterns are discernable within the residuals and an even spread of error is indicated. The relationship is expressed as follows (where the per mille value of $\delta^{18}O_A$ is meant):

$$CAI = (-40.27\delta^{18}O_A + 43.12)^2$$

Because our CAI–$\delta^{18}O_A$ relationship was developed using best-track records for 1990–2010, our model is not likely to be subject to the degree of intensity bias generated by changes in observational techniques. Nonetheless, when the period of investigation is extended to include 1970–2010, the relationship between CAI and $\delta^{18}O_A$ still holds ($r = -0.5$ (Pearson's correlation coefficient), $P = 0.0001$, $n = 60$) and the average difference in model estimates of CAI is 10^3 that is, less than half the r.m.s.e. of the model. In addition, CAI after 1990 is modelled from $\delta^{18}O$ and is therefore not subject to the same errors noted previously in the pre-1990 instrumental and historical data sets.

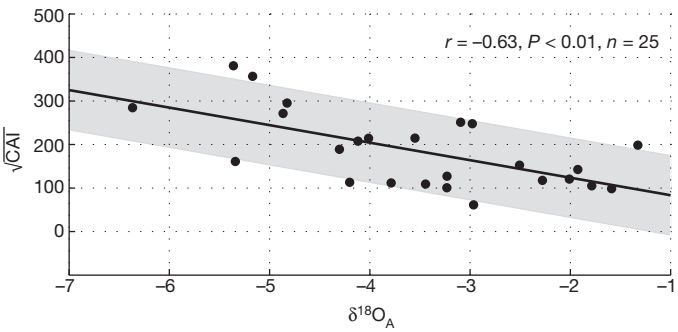

Figure 2 | Calculated CAI versus the de-trended carbonate values from CR-1 and CH-1 ($\delta^{18}O_A$). Grey region indicates the root mean squared error (r.m.s.e.) of the model (difference between actual and modelled CAI values for 1970–2010). $r = 0.63$, $P \leq 0.01$, $n = 25$.

Figure 3a and Fig. 3c give the calculated CAI values over the past 1,500 and 700 years at Cape Range and Chillagoe, respectively. Although it is clear from the analysis of instrumental records that the west coast of Australia is more prone to tropical cyclones than the east coast[24,25], our data indicate that this is not a recent phenomenon. Tropical cyclone activity on the mid west coast of Australia is on average three times higher than on the northeast coast, with CAI values ranging from 10^4 to 1.3×10^5 at Cape Range compared with CAI values of 0.25×10^4 to 1.2×10^5 at Chillagoe. Analysis of CAI indicates that tropical cyclone activity has been highly variable over the past 1,500 years and that tropical cyclone activity in the past was higher than it is today. There has been significantly less tropical cyclone activity at Chillagoe in the past century than in the previous 550 years ($Z = 24.73$ (Z-test statistic),

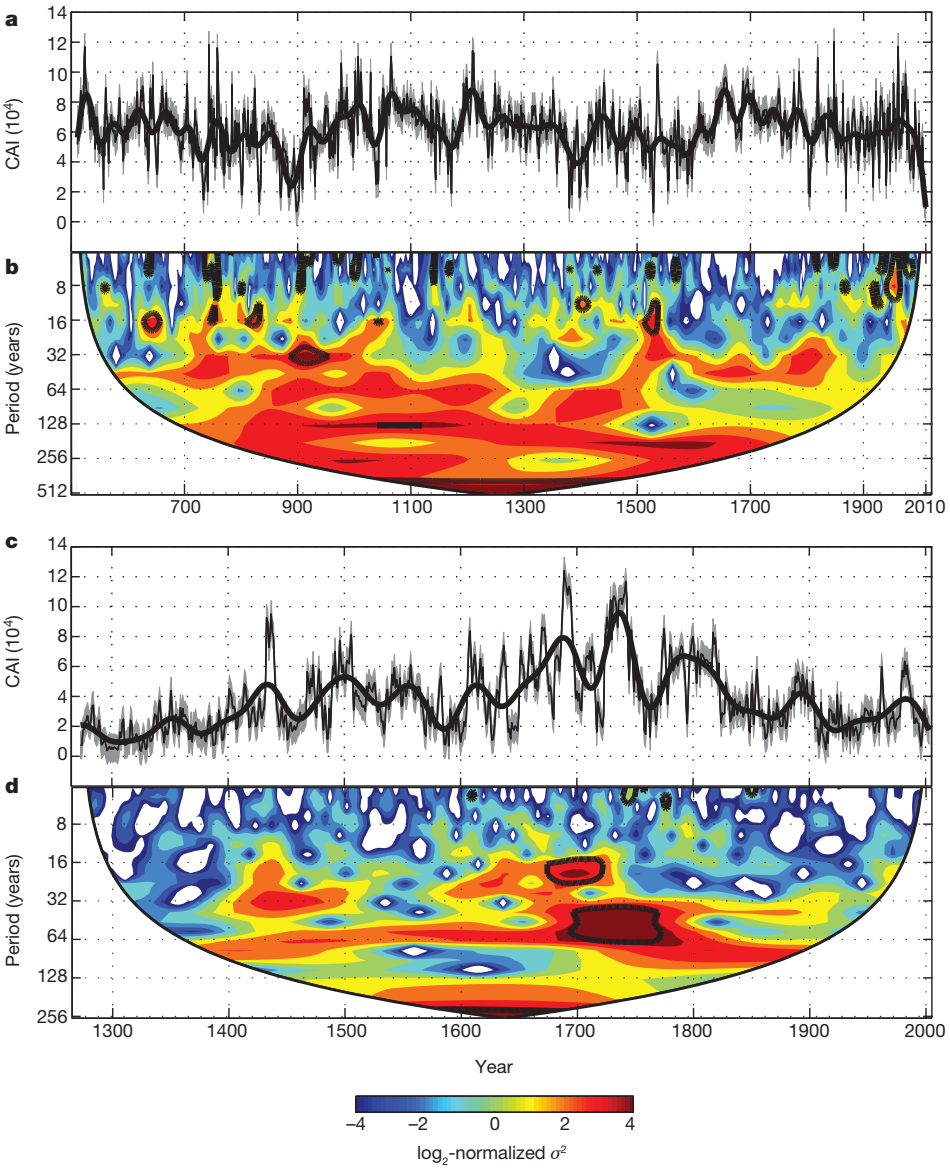

Figure 3 | CAI over the last 1,500 and 700 years. **a**, **c**, Cape Range (**a**) and Chillagoe (**c**); black line indicates smoothing of the series using ref. 31 (smoothed data were not used in the statistical analysis). Grey shading indicates the r.m.s.e. of the model. Four values, which were more than 1 s.d. outside the $\delta^{18}O_A$ range specified in Fig. 1, were removed from the series. **b**, **d**, Wavelet power spectra (Morlet wavelet) of Cape Range (**b**) and Chillagoe (**d**). Power increases from blue to red, black contours indicate regions above the 95% confidence level, and the white areas are regions subject to edge effects. The spectra have lag-1 autocorrelation coefficients of 0.75 (Cape Range) and 0.78 (Chillagoe). Software provided by C. Torrence and G. Compo (http://atoc.colorado.edu/research/wavelets/).

$P < 0.001$). At Cape Range, tropical cyclone activity since 1970 has been significantly lower than it was during the 1,460 years prior ($Z = 22.42$, $P < 0.001$). Wavelet analysis of the time series (Fig. 3b) indicates a reduction in the variance of CAI between the mid 1800s and today at Cape Range within the 16–128-year band. It also highlights an increase in variability within the 4–8-year band before 1960 (although at relatively low power). Significance testing indicates that the majority of the oscillations occur within the 4–32-year frequency band, although the emergence of a 128-year oscillation is indicated between ~AD 1100 and ~1200 and again between ~1400 and ~1600 (however, there is less than 95% confidence in the evidence for the latter). Figure 3c indicates that, relative to the rest of the time series, the variability at Chillagoe was limited during the period before 1400 and after 1900. Significant variations in power are evident between 1700 and 1800 within the 16–64-year band, during which time CAI at Chillagoe was highest (Fig. 3d).

We assessed the rate of the decline in activity over the past few centuries at both sites by conducting a Mann–Kendall test in conjunction with a Theil–Sen estimator. Serial correlation was accounted for by removing the lag-1 autoregressive process after computing the lag-1 serial correlation coefficients for both data sets. Chillagoe shows a significant decline in activity towards the present day since AD 1743 ($\tau = -0.4$ (Kendall's tau), $P < 0.001$, $n = 262$); similarly, an overall decline in activity is seen at Cape Range since 1650 ($\tau = -0.4$, $P < 0.001$, $n = 360$). A more abrupt decline at Cape Range since 1960 is evident in Fig. 3. We assessed this period in relation to the rest of the Cape Range record using a sliding window of 50 years with a 1-year step. The significant downward trend since 1960 is unprecedented in the Cape Range record ($\tau = -0.5$, $P < 0.001$, $n = 50$). These factors in conjunction suggest that the modern instrumental era (1970–2010) provides a poor reflection of the true natural variability of tropical cyclone activity in both regions.

Trend analysis of instrumental data globally has shown a reduction in frequency in all basins[26] (excluding the Atlantic[6,27]) but in many cases an increase in the number and proportion of severe tropical cyclones[26]. Within the Australian region, the downward trend in tropical cyclone

activity over the past 30 years on the east[28] and west coasts[25] is in contrast to reports of no trend[4]. It has been suggested that the downward trend noted in the former studies is probably due to an improvement in the ability to differentiate tropical cyclones from severe tropical lows and to the greater number of El Niño events since 1970[29].

We performed a Mann–Kendall trend test within both the Chillagoe and the Cape Range data sets on the timescales used in the studies referred to above. Our results agree with those of ref. 4 in that no significant trends in tropical cyclone activity in central Western Australia are indicated within the period 1980–2007 ($\tau = -0.2$, $P = 0.103$); however, a significant decrease in activity is evident when the period of investigation is extended beyond the past 30 years (as previously noted). Similarly, our results are also in agreement with those of an analysis of the Eastern Australian region from 1870–2010, showing a distinct downward trend in tropical cyclone activity in northeast Queensland[28] ($\tau = -0.4$, $P < 0.001$).

The Australian region seems to be experiencing the most pronounced phase of tropical cyclone inactivity for the past 550–1,500 years. The dramatic reductions in activity since the industrial revolution suggest that climate change cannot be ruled out as a causative factor. This reduction is also in line with present projections for the late twenty-first century from global climate models, yet our results suggest that this is occurring much sooner than expected. However, we cannot say whether this downward trend in activity will be sustained.

We anticipate that CAI will be a starting point for more sophisticated analysis of other palaeotempest records from around the globe as potential inputs for regional or global climate models and long-range statistical or dynamical forecast models. Deriving a scale of tropical cyclone activity from established high-resolution climate palaeorecords such as stalagmites makes it possible to examine tropical cyclone activity on multiple temporal scales in conjunction with other climate indices, such as temperature, atmospheric CO_2 concentrations, El Niño/Southern Oscillation, the Madden–Julian Oscillation and the Dipole Mode Index. Therefore, CAI provides one seamless index allowing for the incorporation of much longer tropical cyclone records into climate or forecasting models. CAI could be calculated from other stalagmite records and potentially other palaeotempest records from other basins when verified against the local instrumental tropical cyclone record using the method presented here. This provides the means to examine not only how tropical cyclone activity has varied as a result of industrialization but also potentially to forecast future trends in tropical cyclone activity under changing climate conditions, given that it is now possible to discern natural variability from anthropogenically induced change.

METHODS SUMMARY

The most recent 1,500 dark-calcite layers representing wet-season deposition were subsampled using a video-controlled micromill. Oxygen and carbon isotope analyses were performed using a Kiel III carbonate device coupled to a Finnigan MAT 253 IRMS. Each calcite sample was reacted with three drops of H_3PO_4 at 70 °C. Replicate analysis of the standard NBS-19 resulted in a standard deviation of 0.04‰ for $\delta^{13}C$ and 0.06‰ for $\delta^{18}O$. All measurements are reported relative to Vienna PeeDee Belemnite (VPDB). To ensure that the isotopes within the calcite had been deposited in equilibrium with the cave drip water, we conducted a Hendy test for equilibrium deposition at 4.09 and 16.2 cm from the apices of CH-1 and CR-1, respectively. Four or five subsamples were milled for each test at 2–5-mm intervals along the growth horizon from the centre of the layer toward the flanks. Both stalagmites pass Hendy's first test for equilibrium[30] because the maximum variation in $\delta^{18}O$ across the layer is less than 0.8‰ (specifically 0.27‰ for CH-1 and 0.61‰ for CR-1) and neither stalagmite exhibits progressive enrichment in either $\delta^{18}O$ or $\delta^{13}C$ towards the flanks.

Online Content Any additional Methods, Extended Data display items and Source Data are available in the online version of the paper; references unique to these sections appear only in the online paper.

Received 19 June; accepted 14 November 2013.

1. Knutson, T. R. *et al.* Tropical cyclones and climate change. *Nature Geosci.* **3,** 157–163 (2010).
2. Nott, J. & Hayne, M. High frequency of 'super-cyclones' along the Great Barrier Reef over the past 5,000 years. *Nature* **413,** 508–512 (2001).
3. Landsea, C. W., Harper, B. A., Hoarau, K. & Knaff, J. A. Climate change: can we detect trends in extreme tropical cyclones? *Science* **313,** 452–454 (2006).
4. Harper, B. A., Stroud, S. A., McCormack, M. & West, S. A. A review of historical tropical cyclone intensity in north-western Australia and implications for climate change trend analysis. *Aust. Meteorol. Mag.* **57,** 121–141 (2008).
5. Kamahori, H., Yamazaki, N., Mannoji, N. & Takahashi, K. Variability in intense tropical cyclone days in the western North Pacific. *SOLA* **2,** 104–107 (2006).
6. Emanuel, K. Increasing destructiveness of tropical cyclones over the past 30 years. *Nature* **436,** 686–688 (2005).
7. Emanuel, K., Sundararajan, R. & Williams, J. Hurricanes and global warming: results from downscaling IPCC AR4 simulations. *Bull. Am. Meteorol. Soc.* **89,** 347–367 (2008).
8. Elsner, J. B., Kossin, J. P. & Jagger, T. H. The increasing intensity of the strongest tropical cyclones. *Nature* **455,** 92–95 (2008).
9. Oouchi, K. *et al.* Tropical cyclone climatology in a global-warming climate as simulated in a 20 km-mesh global atmospheric model: frequency and wind intensity analyses. *J. Meteorol. Soc. Jpn* **84,** 259–276 (2006).
10. Zhao, M., Held, I. M., Lin, S. J. & Vecchi, G. A. Simulations of global hurricane climatology, interannual variability, and response to global warming using a 50-km resolution GCM. *J. Clim.* **22,** 6653–6678 (2009).
11. Abbs, D. *The Impact of Climate Change on the Climatology of Tropical Cyclones in the Australian Region*. CAF Working Paper 11 (CSIRO, 2010).
12. Nicholls, N., Landsea, C. & Gill, J. Recent trends in Australian region tropical cyclone activity. *Meteorol. Atmos. Phys.* **65,** 197–205 (1998).
13. Kossin, J. P. *et al.* A globally consistent reanalysis of hurricane variability and trends. *Geophys. Res. Lett.* **34,** L04815 (2007).
14. Bell, G. D. *et al.* Climate Assessment for 1999. *Bull. Am. Meteorol. Soc.* **81,** 1328 (2000).
15. Yu, J. Y., Chou, C. & Chiu, P. G. A revised accumulated cyclone energy index. *Geophys. Res. Lett.* **36,** L14710 (2009).
16. Kantha, L. Time to replace the Saffir-Simpson hurricane scale? *Eos* **87,** 3–6 (2006).
17. Gedzelman, S., Lawrence, J., Gamache, J. & Black, M. Probing hurricanes with stable isotopes of rain and water vapor. *Mon. Weath. Rev.* **131,** 1112–1127 (2003).
18. Lawrence, J. R., Gedzelman, S. D., Zhang, X. & Arnold, R. Stable isotope ratios of rain and vapor in 1995 hurricanes. *J. Geophys. Res.* **103,** 11381–11400 (1998).
19. Frappier, A. B. *et al.* Stalagmite stable isotope record of recent tropical cyclone events. *Geology* **35,** 111–114 (2007).
20. Nott, J., Haig, J., Neil, H. & Gillieson, D. Greater frequency variability of landfalling tropical cyclones at centennial compared to seasonal and decadal scales. *Earth Planet. Sci. Lett.* **255,** 367–372 (2007).
21. Mühlinghaus, C., Scholz, D. & Mangini, A. Modelling fractionation of stable isotopes in stalagmites. *Geochim. Cosmochim. Acta* **73,** 7275–7289 (2009).
22. Griffiths, M. L. *et al.* Increasing Australian-Indonesian monsoon rainfall linked to early Holocene sea-level rise. *Nature Geosci.* **2,** 636–639 (2009).
23. Bureau of Meteorology. Australian Tropical Cyclone Database. *Previous Tropical Cyclones* (12 March 2012).
24. Liu, K. S. & Chan, J. C. L. Interannual variation of Southern Hemisphere tropical cyclone activity and seasonal forecast of tropical cyclone number in the Australian region. *Int. J. Climatol.* **32,** 190–202 (2012).
25. Hassim, M. E. E. & Walsh, K. J. E. Tropical cyclone trends in the Australian region. *Geochem. Geophys. Geosyst.* **9,** Q07V07 (2008).
26. Webster, P. J., Holland, G. J., Curry, J. A. & Chang, H. R. Changes in tropical cyclone number, duration, and intensity in a warming environment. *Science* **309,** 1844–1846 (2005).
27. Mann, M. E. & Emanuel, K. A. Atlantic hurricane trends linked to climate change. *Eos Trans. AGU* **87,** 233–241 (2006).
28. Callaghan, J. & Power, S. Variability and decline in the number of severe tropical cyclones making land-fall over eastern Australia since the late nineteenth century. *Clim. Dyn.* **37,** 647–662 (2011).
29. Braganza, K. *et al.* in *Climate Science Update: A Report to the 2011 Garnaut Review* (eds Keenan, T. D. & Cleugh, H. A.) 3–16 (Centre for Australian Weather and Climate Research, 2011).
30. Hendy, C. H. The isotopic geochemistry of speleothems–I. The calculation of the effects of different modes of formation on the isotopic composition of speleothems and their applicability as palaeoclimatic indicators. *Geochim. Cosmochim. Acta* **35,** 801–824 (1971).
31. Mann, M. E. Smoothing of climate time series revisited. *Geophys. Res. Lett.* **35,** L16708 (2008).

Supplementary Information is available in the online version of the paper.

Acknowledgements Funding for this project was provided by the Australian Research Council (ARC) Discovery Projects Scheme (reference number DP0772691) and financial assistance given as part of the Queensland Smart State Initiative. Analytical procedures were conducted at James Cook University and the University of Utrecht. Special thanks are extended to C. Zwart for his input and advice regarding the development of CAI and his editing of this manuscript. Additional thanks are extended to A. van Dijk and L. Lourens for technical help with IRMS analyses.

Author Contributions J.N. collected the two stalagmites, provided funding for the project through the ARC grant and participated in critical discussions on the

development of CAI. G.-J.R. provided access to facilities and advice on the data processing. J.H. helped collect one stalagmite, processed both stalagmites, analysed the data, developed and tested CAI, and wrote the manuscript. All authors discussed the results and commented on the manuscript.

Author Information Reprints and permissions information is available at www.nature.com/reprints. The authors declare no competing financial interests. Readers are welcome to comment on the online version of the paper. Correspondence and requests for materials should be addressed to J.H. (jordahna.haig@jcu.edu.au).

METHODS

Analytical procedures. The most recent 1,500 dark-calcite layers representing wet-season deposition were subsampled using a video-controlled micromill. Oxygen and carbon isotope analyses were performed using a Kiel III carbonate device coupled to a Finnigan MAT 253 IRMS. Each calcite sample was reacted with three drops of H_3PO_4 at 70 °C. Replicate analysis of the standard NBS-19 resulted in a standard deviation of 0.04‰ for $\delta^{13}C$ and 0.06‰ for $\delta^{18}O$. All measurements are reported relative to Vienna PeeDee Belemnite (VPDB). To ensure that the isotopes within the calcite had been deposited in equilibrium with the cave drip water, we conducted a Hendy test for equilibrium deposition at 4.09 and 16.2 cm from the apices of CH-1 and CR-1, respectively. Four or five subsamples were milled for each test at 2–5-mm intervals along the growth horizon from the centre of the layer toward the flanks. Both stalagmites pass Hendy's first test for equilibrium[30] because the maximum variation in $\delta^{18}O$ across the layer is less than 0.8‰ (specifically 0.27‰ for CH-1 and 0.61‰ for CR-1) and neither stalagmite exhibits progressive enrichment in either $\delta^{18}O$ or $\delta^{13}C$ towards the flanks.

CAI formulation. We calculate $K_{n,t}$ for each tropical cyclone that passes within 400 km of either of the two sites, at each observation point along its path since genesis. $K_{n,t}$ is cumulative, and so reflects not only the condition of the system at time t but also its history up until that point:

$$K_{n,t} = (K_t + K_{t-1})_n$$

$$K_t = \frac{V_{\max}^3(t) R_{\max}(t)}{d(t)}$$

Here n enumerates the individual storms, t denotes time along the storm track (recorded at 6-h intervals), d denotes the distance from the site in kilometres at time t, $V_{\max}$ is the maximum 10-min-mean wind speed in metres per second at time t, and $R_{\max}$ is the radius of maximum wind in kilometres at time t.

The resulting $\delta^{18}O$ of the stalagmite carbonate is an average of the collective precipitation events over a season, and we therefore average rather than sum the resulting $K_{n,t}$ values. Thus, CAI is the average accumulated energy expended over the tropical cyclone season within range of the site, accounting for the number of days since genesis of the storm and the intensity and size of the storm relative to its distance from the site at each point in time:

$$\mathrm{CAI} = \frac{1}{N}\sum_{n=1}^{N} K_n$$

Here N is the number of storms within the season.

CAI differs from the accumulated cyclone energy index, the revised accumulated cyclone energy index, the power dissipation index and the hurricane intensity index in that it is tailored to reflect the effects of tropical cyclone activity on the resulting $\delta^{18}O$ of the carbonate layers. CAI is location specific (that is, it accounts for the distance between the site and the centre of the storm track) and gives an average of these tropical cyclone events rather than the sum of the total energy expelled within a season. Because tropical cyclone $\delta^{18}O$ precipitation values are radially asymmetrical within a storm (Extended Data Fig. 1), the inclusion of distance in the calculation of K_t has a dampening effect on the resulting K_n value of that storm with increasing distance. As such, a tropical cyclone located 400 km from the study site at $K_{t=1}$, is weighted less than when located 200 km from the site at $K_{t=2}$, given the same $V_{\max}$ and $R_{\max}$. $K_{n,t}$ does not, however, take into account the angle of approach (for example, the parameter d does not take into account the orientation of the system relative to the study site and does not distinguish between approach or retreat of the system).

***K_t* versus $\delta^{18}O$ VSMOW.** In the absence of tropical cyclone rainfall measurements in Australia, to test how well K_t is reflected in the $\delta^{18}O$ of tropical cyclone precipitation we calculated the corresponding K_t values for Hurricane Olivia (a 1994 eastern North Pacific hurricane) using the NHC's updated HURDAT Best Track Database[32]. These were compared against $\delta^{18}O$ VSMOW measurements[33] made at 30-min intervals between 24 and 26 September 1994. The results are plotted in Extended Data Fig 1. We find that $\delta^{18}O$ depletion increases with increasing K_t ($\rho = -0.5$, $P = 0.02$, $n = 25$), supporting our derivation of K_t and, thus, CAI. Within the eyewall (the ring or belt of thunderstorms surrounding the central eye within the radius of maximum wind), $R_{\max}$ is statistically not significant, K_t in Extended Data Fig. 1b is therefore calculated as a function of $V_{\max}$ and distance alone.

De-trending monsoon. Because tropical cyclone rainfall accounts for only 20.05% and, respectively, 17% of the total rainfall at Chillagoe and Cape Range, it is necessary to exclude the average monsoonal component of the stalagmite carbonate ($\delta^{18}O_M$). We estimated $\delta^{18}O_M$ at Chillagoe and Cape Range using.

$$\delta^{18}O\,(‰) = -0.005 \times \mathrm{Longitude}\,(^\circ) - 0.034 \times \mathrm{Latitude}\,(^\circ) - 0.003 \times \mathrm{Altitude}\,(\mathrm{m}) - 4.753 \quad (1)$$

(adjusted $R^2 = 0.79$) and

$$\delta^{18}O = (6.67 \times 10^{-6})P^2 - 0.009P + 0.015 \times \mathrm{Eva} + 0.007 \times \mathrm{Rad} - 9.670 \quad (2)$$

(adjusted $R^2 = 0.645$), which are empirical equations for geographical (equation (1)) and local (equation (2)) meteorological controls on $\delta^{18}O$ derived from an analysis of Global Network of Isotopes in Precipitation (GNIP) and instrumental meteorological data[34]. Here P is total monthly precipitation, Eva is average monthly evaporation and Rad is average monthly radiation. Rainfall events 3 days on either side of a tropical cyclone event within 400 km of our sites were excluded from our calculations. It is important to note that Liu's geographical model does not take into account factors such as the source region, transport and condensation history of the air masses. Precipitation at Chillagoe is derived from sources in the Coral Sea and the Gulf of Carpentaria. These may have originally been part of a larger air mass, which has travelled north from cooler waters or south from warmer waters. In contrast, precipitation at Cape Range is largely derived from oceanic air masses from the Indian Ocean. However, at this stage there are no other longitudinal, in-depth analyses of $\delta^{18}O$ in precipitation from the east or west coast of Australia excepting the model used here from ref. 34. Using this relationship and local historical climate data from the two sites, we calculated the average seasonal $\delta^{18}O_M$ VSMOW from 1990 to 2010. $\delta^{18}O_M$ was then normalized and used to de-trend the modern $\delta^{18}O$ to remove the modern monsoonal trend. $\delta^{18}O_M$ beyond the instrumental record was de-trended from the $\delta^{18}O$ data using a spline-interpolated, normalized data set generated from an established Australian–Indonesian monsoonal proxy record[22]. This record has a resolution of ~10 years and extends from 7 years BP to 12,000 years BP, the region experiences a relatively low tropical cyclone frequency (on average, 0.24 tropical cyclones per year pass within 400 km of the site[23]), and the record is comparable with other established monsoonal records from the region[22].

CAI calculation from the Australian tropical cyclone database. From the period 1990–2010, CAI values for Chillagoe and Cape Range were calculated within 400 km of each site using the data available within the Australian Bureau of Meteorology's tropical cyclone database[23]. Of the tropical cyclones recorded within the database, 32 and 35 passed within 400 km of Chillagoe and Cape Range, respectively. Of the 2,114 observation points within the combined data sets, 225 do not contain wind speed measurements. Given the limited number of environmental pressure measurements available, $V_{\max}$ was estimated using the Atkinson/Holliday wind–pressure relationship[35]:

$$V_{\max} = 0.514[6.7(1{,}010 - P_c)^{0.644}] \quad (3)$$

Here P_c is the central pressure in millibars and $V_{\max}$ is the maximum 10-min-mean wind speed in metres per second. There was an average discrepancy of 3 m s^{-1} between the value of $V_{\max}$ estimated using equation (3) and the recorded $V_{\max}$ (Dvorak technique[36]) within the remaining 1,889 observations. Missing $R_{\max}$ estimates from 1,702 observations were calculated using[37]

$$R_{\max} = 46.4 \exp(-0.0155 V_{\max} + 0.0169\varphi)$$

An average discrepancy of 17.5 km was found between the measured and estimated values.

32. NOAA. HURDAT Best Track Data. *NOAA Hurricane Research Division of AOML* http://www.aoml.noaa.gov/hrd/hurdat/tracks1949to2011_epa.html (13 March 2013).
33. Lawrence, J. R., Gedzelman, S. D., Gamache, J. & Black, M. Stable isotope ratios: Hurricane Olivia. *J. Atmos. Chem.* **41,** 67–82 (2002).
34. Liu, J. *et al.* Stable isotopic compositions in Australian precipitation. *J. Geophys. Res.* **115,** D23307 (2010).
35. Atkinson, G. D. & Holliday, C. R. Tropical cyclone minimum sea level pressure/maximum sustained wind relationship for the western North Pacific. *Mon. Weath. Rev.* **105,** 421–427 (1977).
36. Velden, C, *et al.* The Dvorak tropical cyclone intensity estimation technique: a satellite-based method that has endured for over 30 years. *Bull. Am. Meteorol. Soc.* **87,** 1195–1210 (2006).
37. Willoughby, H. E. & Rahn, M. E. Parametric representation of the primary hurricane vortex. Part I: Observations and evaluation of the Holland (1980) model. *Mon. Weath. Rev.* **132,** 3033–3048 (2004).

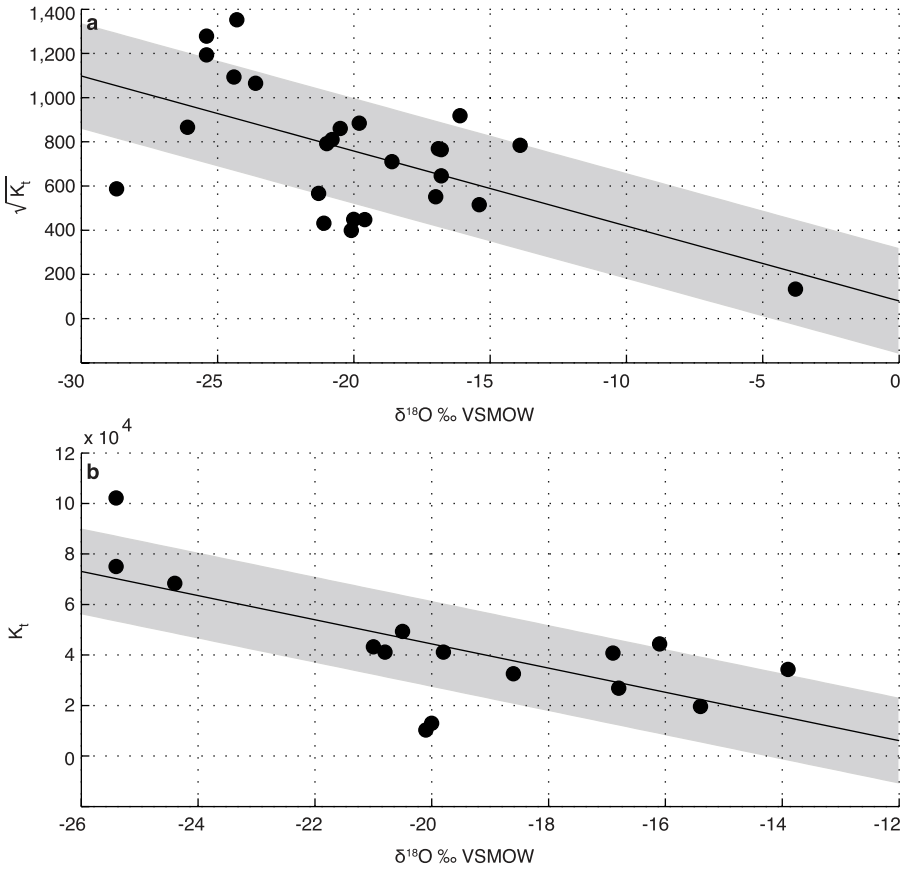

Extended Data Figure 1 | δ^{18}O VSMOW measured from Hurricane Olivia (1995) versus the calculated K_t values for the corresponding measurement interval. **a**, δ^{18}O versus K_t for all rain types in Hurricane Olivia. $r = -0.58$, $P = 0.02$, $n = 25$. **b**, δ^{18}O versus K_t within the eye wall. Shaded area indicates the r.m.s.e. $r = -0.70$, $P = 0.02$, $n = 15$.